polymer papers

Rod aggregation in graft rigid-rod copolymers for single-component molecular composites

H. H. Song*, M. Dotrong, G. E. Price and M. H. Dotrong
University of Dayton Research Institute, Dayton, OH 45469, USA

and U. M. Vakil and U. Santhosh
AdTech Systems Research Inc., Dayton, OH 45432, USA

and R. C. Evers
Wright Laboratory, Wright-Patterson Air Force Base, OH 45433, USA

Graft copolymers of rigid-rod polymers, specially synthesized for single-component molecular composites, were investigated by wide-angle X-ray scattering. The copolymers consist of a flexible poly(ether ketone) (PEK) side chain attached to a rigid-rod poly(p-phenylene benzobisthiazole) (PBZT). Emphasis was espcially placed on the extent of rod aggregation in the copolymers before and after heat treatments. Results were compared among the graft copolymers of various structural characteristics and the blend of PBZT and PEK homopolymers. The results confirmed that the flexible side chains effectively suppress the thermally induced rod aggregation. The frequency of the graft sites along the rigid-rod backbone was found to be the key structural parameter limiting the extent of rod aggregation. A certain minimum frequency of the graft sites appeared to be required for the copolymers to be stable against the thermal aggregation. The side-chain length showed only a minimal effect, while the rigid-rod backbone length exhibited no effect on the stability of the copolymer morphology in association with the thermal aggregation.

(Keywords: graft rigid-rod copolymer; molecular composite; wide-angle X-ray scattering)

INTRODUCTION

Composite micromechanics[1,2] predicts that maximum reinforcement in a fibre and matrix composite can be achieved by maximizing the aspect ratio of the reinforcing fibre, i.e. by either extending the fibre to an infinite length or reducing its cross-section to a molecular level. Based on this theoretical background, the concept of a rigid-rod molecular composite was proposed at the Air Force Materials Laboratory[3]. The basic concept of a molecular composite is to develop a material consisting of a rigid-rod polymer dispersed in a flexible-coil polymer matrix, where the maximum reinforcement is achieved if the dispersion occurs at the molecular level.

Among a number of polymer systems investigated, the first successful system[4] was a blend of rigid-rod poly(p-phenylene benzobisthiazole) (PBZT) in a flexible poly[2,5(6)-benzimidazole] or in a flexible poly(2,6-benzothiazole). The polymer blends revealed a minimal phase separation of very small scale aggregation (less than ~5 nm)[5] and exhibited excellent mechanical properties, confirming the original concept of the molecular composite. The aromatic heterocyclic system, however, is intractable and can only be processed in solutions of strong acid such as methanesulfonic acid

(MSA). The efforts were then directed to develop a thermoplastic matrix system having the ability to be moulded into a bulk form. Numerous systems[6–9] consisting of rigid-rod and thermoplastic polymers have been investigated. However, there are common fundamental difficulties in the processing of these polymer blends associated with the incompatibility of rods and coils. Incompatibility between rods and coils, having its origin in the low entropy of mixing, causes extensive phase separation during the thermal processing, thus resulting in a significant lowering of reinforcement efficiency. Research efforts[10–13] were consequently focused on modification of the polymer structure to improve the compatibility between the rods and coils and/or to disturb the ordering of the rods sterically, and thus limit the rod aggregation.

Recently, graft copolymers consisting of a long, flexible poly(ether ketone) (PEK) side chain attached to a rigid-rod PBZT backbone were synthesized in our laboratory. The main objective was to utilize the long, flexible side chains not only to limit the rod aggregation but also to serve as the thermoplastic matrix, i.e. to make a single-component molecular composite. The polymer synthesis[14] and the processing and mechanical properties[15] of the copolymers have already been published elsewhere. In this paper, we focus on the extent of rod aggregation in the graft copolymers having

* To whom correspondence should be addressed

various structural characteristics. Wide-angle X-ray scattering (WAXS) was used as the main technique to analyse the extent of rod aggregation and scanning electron microscopy (SEM) was also used to examine the polymer morphology on a larger scale.

EXPERIMENTAL

Materials and sample preparation

Five polymer samples, four copolymers and one physical blend of PBZT and PEK, were used in this study. The chemical structure of the copolymer is shown in *Figure 1* and the structural characteristics of the five samples are summarized in *Table 1*. The graft sites of the copolymers are assumed to be randomly distributed along the PBZT backbone. The copolymer composition was determined from the mass balance of the initial PBZT and the resulting graft copolymer. The intrinsic viscosities of the samples shown in *Table 1* were obtained from the samples before the side-chain attachment. The viscosities, therefore, represented the molecular weights of the PBZT polymer backbones. The calculated[16] average lengths of the PBZT backbones were ~ 90 nm for the graft copolymers C1, C3, and C4 and ~ 40 nm for the graft copolymer C2. The side-chain lengths listed in the last column of *Table 1* were then derived from the two given parameters, i.e. graft sites (mol%) and compositions.

The copolymers and the blend were obtained by precipitating very dilute polymer solutions (below the critical concentration of PBZT in MSA) in water. The precipitated polymers were isolated by filtration, washed with dilute NH_4OH and subsequently with water. The polymers were then dried in vacuum at 100°C. Non-heat-treated polymer samples used for the X-ray scattering were all in powder form. Heat-treated graft copolymers were all compression moulded at elevated temperatures, while the blend was heat treated in powder form.

X-ray scattering and scanning electron microscopy

Wide-angle X-ray intensities were measured by a Picker diffractometer coupled to a Rigaku RU 200 rotating-anode X-ray generator ($CuK\alpha$) operating at 45 kV and 70 mA. The X-ray beam was collimated by two pinholes and was monochromated by a Ni filter. Scattered X-ray intensities from $S\,(=2\,\sin(\theta/\lambda))=0.6\,\mathrm{nm}^{-1}$ to $9.2\,\mathrm{nm}^{-1}$ were collected by a scintillation counter. Here 2θ denotes the scattering angle and λ the X-ray wavelength. A number of corrections (background, polarization, Compton scattering and absorption) were applied to the raw X-ray intensities before further analysis was made.

Freeze-fractured surfaces of the copolymers were also examined by a field emission, high-resolution scanning electron microscope (Hitachi S-900). The specimens were prepared by fracturing the samples at liquid nitrogen temperature.

RESULTS AND DISCUSSION

X-ray intensities were measured from a 50/50 blend of PBZT and PEK and the graft copolymers C1, C2, C3, and C4 both before and after heat treatment. The heat treatment temperatures were 125, 200, and 300°C for the blend; 230 and 300°C for C1; 300°C for C2; 200, 250, and 300°C for C3; and 200 and 250°C for C4. Representative X-ray intensities are plotted in *Figures 2* to *6*, respectively.

Before discussing the X-ray intensities of the copolymers and blend, we begin with the individual wide-angle X-ray intensities of PBZT and PEK homopolymers. In

Figure 1 Chemical structure of the graft copolymer PBZT-*g*-PEK

Table 1 Structural characteristics of graft copolymers and the blend

Sample	Graft sites (mol%)	$[\eta]^a$ PBZT	PBZT/PEK (w/w)	PEK repeat unit (n)
Blend	0	16	50/50	–
C1	10	8.6	46/54	17
C2	10	4.3	52/48	13
C3	30	8.3	53/47	5
C4	30	8.3	29/71	13

^{a} Measured in methanesulfonic acid at 30°C
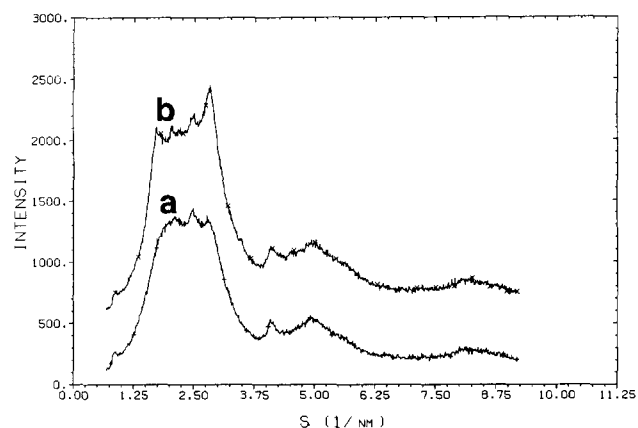
Figure 2 Wide-angle X-ray intensities of the 50/50 blend of PBZT and PEK (a) before and (b) after heat treatment at 300°C
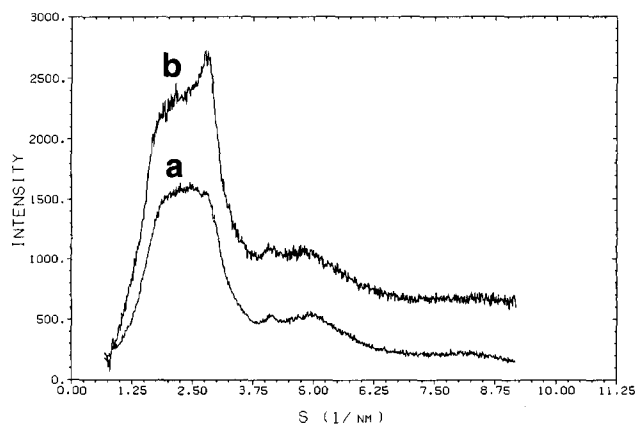
Figure 3 Wide-angle X-ray intensities of copolymer C1 (a) before and (b) after heat treatment at 300°C
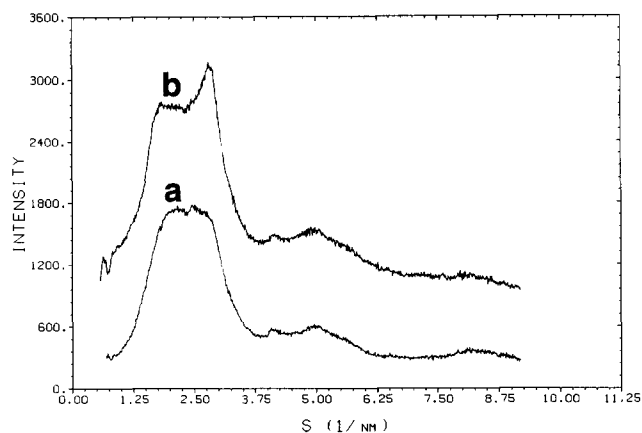
Figure 4 Wide-angle X-ray intensities of copolymer C2 (a) before and (b) after heat treatment at 300°C
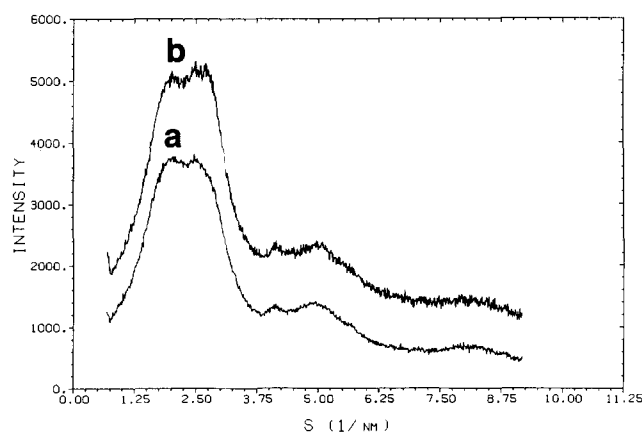
Figure 5 Wide-angle X-ray intensities of copolymer C3 (a) before and (b) after heat treatment at 250°C
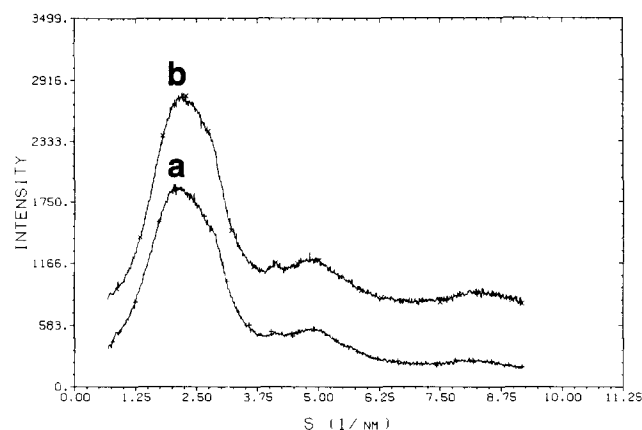
Figure 6 Wide-angle X-ray intensities of copolymer C4 (a) before and (b) after heat treatment at 250°C

Figure 7, the X-ray intensities from a PBZT powder are shown. Two main peaks at $S = 1.7 \, \text{nm}^{-1}$ and $2.8 \, \text{nm}^{-1}$ and several other weak but rather sharp peaks are noticed. The two main peaks are from the interchain packing of the PBZT molecules and can be assigned to (200) and (010) reflections according to the crystal structure of PBZT derived by Fratini et al.[17]. The other small peaks are from the intrachain order along the rigid-rod backbone in the extended PBZT polymer chain. A

completely different pattern is observed for the X-ray intensities of PEK, as shown in *Figure 8*. The pattern shows only broad haloes without any diffraction peaks, indicative of the amorphous state of the PEK polymer.

The X-ray intensities of a binary system $I_C(S)$ can be expressed as

$$I_C(S) = \alpha I_A(S) + \beta I_B(S) + \gamma I_{AB}(S) \qquad (1)$$

where $I_A(S)$ and $I_B(S)$ are the X-ray intensities of the individual components and $I_{AB}(S)$ is a cross-term arising from the correlation between the two components. The significance of the cross-term is dependent on both the morphology of the binary system and the scattering angles (S) of interest. In a phase-separated binary system of large domains, the cross-term becomes negligible and the X-ray intensities can be approximated as a superposition of the X-ray intensities of the individual components. Even in a system where the phase domains are small this approximation is still valid, especially at the wide angles where a short correlation distance is concerned. It is quite apparent that the X-ray patterns of the blend and the copolymers shown in *Figures 2* to *6* resemble composite patterns of PBZT (*Figure 7*) and PEK (*Figure 8*) X-ray intensities.

Comparison of the raw X-ray intensities of the copolymers and the blend with the intensities after heat treatment reveals that the thermal responses of the polymer samples differ remarkably, even though the X-ray intensities of all five samples before heat treatment are essentially identical. As can be seen in the X-ray
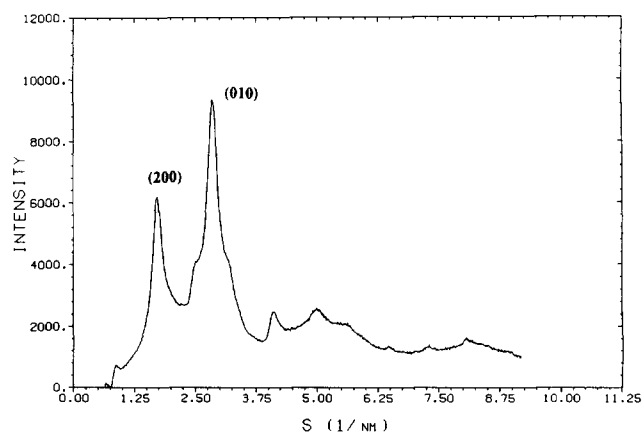
Figure 7 Wide-angle X-ray intensities measured for PBZT powder
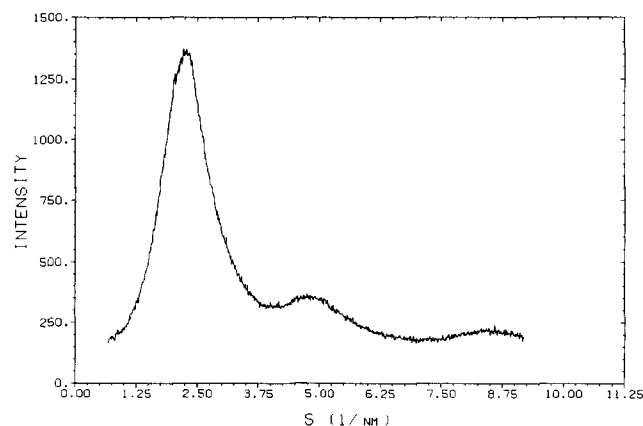
Figure 8 Wide-angle X-ray intensities measured for PEK powder

intensities of the blend (*Figure 2*), the two peaks at $S = 1.7$ nm^{-1} and 2.8 nm^{-1}, which are the two main (200) and (010) reflections arising from the interchain packing of PBZT molecules, become stronger after the heat treatment. The appearance of the two peaks is a clear indication of aggregation of rod molecules induced by the heat treatment at an elevated temperature. Growth of the peak at $S = 2.8$ nm^{-1} can also be observed from the X-ray intensities of the two graft copolymers C1 and C2 shown in *Figures 3* and *4*. The results are indicative of the thermally induced aggregation of rod backbones, even though the copolymers have long, flexible side chains. However, the X-ray intensities of the copolymers C3 and C4, shown in *Figures 5* and *6*, undergo hardly any changes as a result of the heat treatment and no such marked peaks at $S = 1.7$ nm^{-1} and 2.8 nm^{-1} are observed in the features of their X-ray patterns. These results imply that certain structural characteristics in the last two copolymers (C3 and C4) provide stability against thermal aggregation. A common structural difference between the two sets of copolymers can be found in their graft site frequencies. The copolymers C1 and C2 have 10% graft sites along the rigid-rod backbone, while the copolymers C3 and C4 have a higher frequency of 30% graft sites.

Instead of examining the raw X-ray intensities directly, as discussed above, we further analysed the X-ray intensities by decomposing them into the individual intensity components of PEK and PBZT. This was based on our argument that the wide-angle X-ray intensities of the copolymers and the blend can be approximated as composite intensities of the two homopolymers. One example of decomposing the X-ray intensities is shown in *Figure 9*. In this process, the X-ray intensities of PEK scaled according to the volume fraction were first subtracted from the intensities of the blend or the copolymer. The remainder was then subjected to a best-fit analysis to give the diffraction peaks of PBZT. After decomposing the X-ray intensities, the full width at half maximum (*FWHM*) and the integrated intensity (*Q*) of the (010) reflection ($S = 2.8$ nm^{-1}) of PBZT were derived to examine the rod aggregations of the blend and the copolymers. Here the *FWHM*s derived from the X-ray intensities can be used to estimate the extent of rod aggregation using the Scherrer equation[18]. Normalized *Q* factors, on the other hand, defined as

$$Q = \int S^2 I_{(010)}(S)\, dS \Big/ \int S^2 I(S)\, dS \tag{2}$$

can be used to evaluate the extent of rod aggregation in the copolymers and the blend as well as any subsequent changes after heat treatment.

In *Figure 10* the inverse *FWHM*s are plotted against the heat treatment temperatures. All five samples have similar initial *FWHM*s, which in fact is consistent with the results of the raw X-ray intensities discussed above, implying similar morphologies for the samples before the heat treatment. This result also suggests that precipitation of the polymer solution effectively limited the phase separation. The thermal responses of the samples, however, differ greatly as the effect of the flexible side chain is evident in the plot. The blend exhibits a rapid increase of the (010) peak sharpness with increasing heat treatment temperature. Copolymers C1 and C2 with 10% graft sites also show a similar behaviour but with a substantially suppressed rate of increase. Both copolymers with 30% graft sites, one with a

53/47 rod–coil composition (C3) and the other with a 29/71 rod–coil composition (C4), however, remained unchanged throughout the heat treatment up to 285°C.

Comparison of the *Q* values shown in *Figure 11* reveals quite different features from those of the *FWHM*s. The blend and copolymers C1 and C2 with 10% graft sites show growth of *Q* values with heat treatment, which is
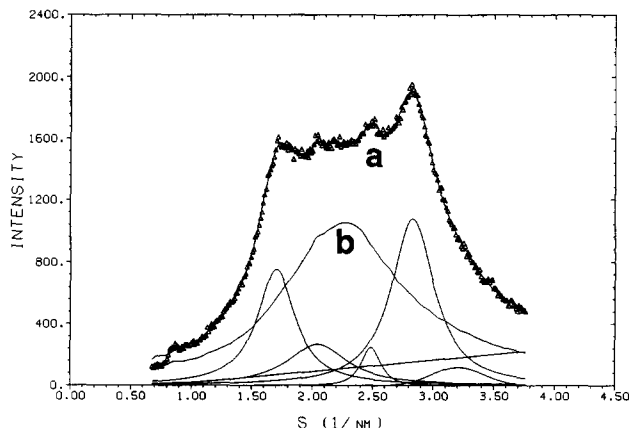
Figure 9 Schematic describing the decomposition of the X-ray intensities of the blend (or copolymer) into the individual intensities of PBZT and PEK. Curves (a) and (b) represent X-ray intensities experimentally obtained from the blend and PEK, respectively. After subtracting curve (b) from curve (a), the remainder was subjected to a best-fit analysis to derive the diffraction peaks of PBZT
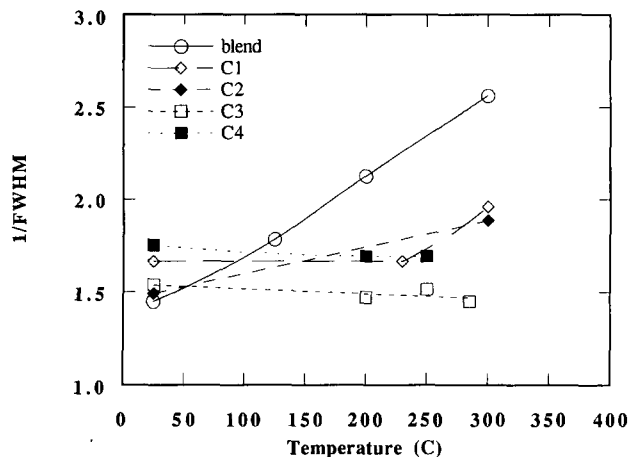
Figure 10 Plot of $1/FWHM$ *versus* heat treatment temperature
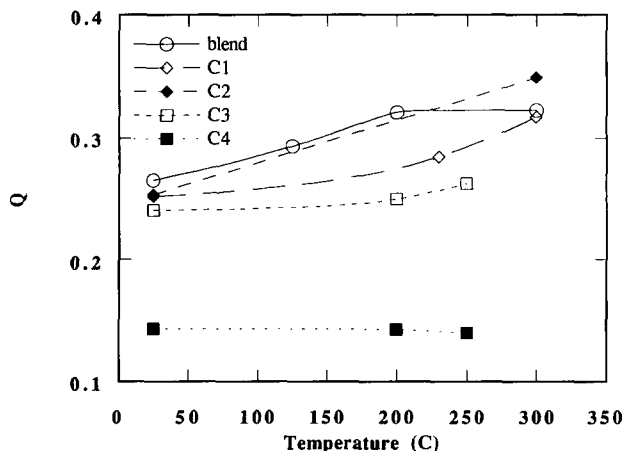
Figure 11 Plot of normalized *Q* *versus* heat treatment temperature

consistent with the *FWHM* results. The blend and the copolymers not only have nearly the same growth rate but their Q values are not significantly different at 300°C. The sharpening of diffraction peaks observed in the physical blend and the copolymers with 10% graft sites could be due either to a true increase in aggregate size or an increase in packing order without any additional thermal aggregation. The increasing Q values noted in the samples confirm a true increase in the aggregate sizes. However, a substantial part of the peak sharpening, especially in the blend, is apparently contributed by the improvement of packing order in the rod domains. Copolymer C3 with 30% graft sites and a 53/47 rod–coil composition also shows a slight increase in Q, indicative of thermally induced aggregation in the copolymer, even though no discernible change was noticed in the *FWHM*. Copolymer C4 with 30% graft sites and a 29/71 rod–coil composition, on the other hand, shows a constant Q value which is consistent with the *FWHM* results.

The results of the raw X-ray intensities and *FWHMs* of the (010) reflection as well as the integrated intensities (Q) clearly indicate that the frequency of the side chains along the rigid-rod backbone plays the most important role in determining the stability of the copolymer morphology. A certain minimum concentration of graft sites along the backbone appears to be required for the copolymers to be stable against thermal aggregation. It is evident from the results for the blend that PBZT and PEK are not a compatible pair. The stable morphology observed for copolymer C4 is not in a thermodynamic equilibrium state but in a quasi-equilibrium state where the side chains perturb the packing of the backbones by filling the spaces between them. Even though a uniform distribution of graft sites along the polymer backbone is assumed for the calculation of the mol% graft sites, it is quite possible that in some copolymers the graft sites might not be uniformly distributed throughout the polymer backbone. Given the equal probability, it is apparent that copolymers with 10% graft sites, compared to those with 30% graft sites, would have a higher chance of having lengthy portions of the backbone without side chains, and thus would show a greater tendency for aggregation of the rigid-rod backbones.

The slight thermal aggregation noticed in copolymer C3, as opposed to the results for copolymer C4, suggests that the side-chain length also influences the stability of the copolymer morphology. Copolymers with short side chains (and therefore a high rod concentration) would have a higher chance of rod to rod contact. However, the effect appears to be only minimal, as suggested by comparison of the results for copolymers C1 and C3. Copolymer C3 having side chains of only five repeat units exhibits a more stable morphology against thermal aggregation than copolymer C1 with side chains of 17 repeat units. In this comparison, frequency effects must have dominated the effects of side-chain length. Almost identical thermal responses were observed for copolymers C1 and C2, even though the backbone length of copolymer C2 is approximately half that of copolymer C1. This result suggests that changing the polymer backbone length might not be an effective way to control the copolymer morphology in association with thermal aggregation.

Even though copolymer C4 exhibits excellent stability against any additional thermal aggregation, the copolymer still reveals aggregation of rod molecules of ~ 1 nm in
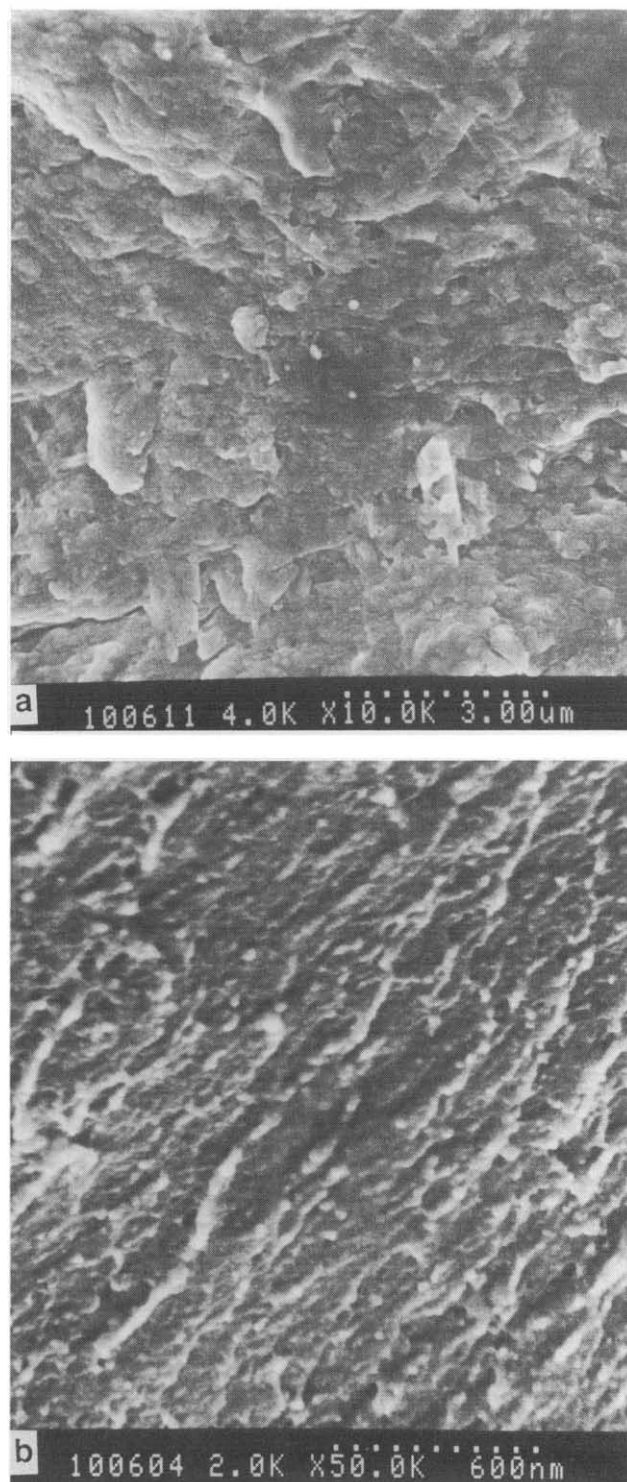
Figure 12 SEM micrographs at two different magnifications obtained from a freeze-fractured surface of copolymer C4 compression moulded at 300°C: (a) $\times 10\,000$; (b) $\times 50\,000$

size, as estimated from Scherrer's equation. The size can be even larger considering the effects of machine broadening and packing disorder. Such aggregation probably originates from the non-uniform distribution of graft sites along the polymer backbone and would have occurred in the solution state or during coagulation.

The results of WAXS discussed so far demonstrate that the long, flexible side chains effectively suppress the rod aggregation and limit the aggregate size to ~ 1 nm. However, a serious question arises if the wide-angle X-ray

technique used for our analyses is used to determine the true domain size of the aggregates. Since the X-ray diffraction measures a coherent crystal stack length across the domain, the possibility of having large domains formed by several crystal stacks cannot be excluded. To confirm the polymer morphology on a larger scale, the copolymers were examined by SEM. Two micrographs at different magnifications obtained from the fractured surface of copolymer C4, which was compression moulded at 300°C, are shown in *Figure 12*. Both micrographs reveal a uniform surface texture without any noticeable domains, thus confirming the very limited phase separation.

CONCLUSIONS

The results, as determined by WAXS, confirm that grafting a long, flexible polymer onto a rigid-rod polymer is an effective approach to limiting rod aggregation. The results also demonstrate the possibility of making a true rigid-rod and flexible-coil molecular composite in bulk form. The frequency of graft sites along the rigid-rod backbone appears to be the key structural parameter in controlling the extent of rod aggregation, especially that occurring during thermal processing. A non-uniform distribution of graft sites along the rigid-rod backbone was interpreted as the origin of both initial aggregation and subsequent thermal aggregation. To overcome the inherent non-uniformity of the graft sites in the random graft copolymers, a certain minimum number of graft sites is required for the copolymers to remain stable at elevated temperatures. The side-chain length variation showed only a minimal effect, while the rigid-rod backbone length exhibited no effect on the stability of the copolymer morphology.

REFERENCES

1   Halpin, J. C. 'Primer on Composite Materials Analysis', Technomic, Lancaster, PA, 1984, Ch. 6
2   Halpin, J. C. and Kardos, J. L. *Polym. Eng. Sci.* 1976, **16**, 344
3   Helminiak, T. E., Benner, C. L., Arnold, F. E. and Husman, G. E. *US Pat. 4207407* 1980
4   Hwang, W.-F., Wiff, D. R., Verschoore, C., Price, G. E., Helminiak, T. E. and Adams, W. W. *Polym. Eng. Sci.* 1983, **23**, 784
5   Krause, S. J., Haddock, T., Price, G. E., Lenhert, P. G., O'Brien, J. F., Helminiak, T. E. and Adams, W. W. *J. Polym. Sci., Polym. Phys. Edn* 1986, **24**, 1991
6   Hwang, W.-F., Wiff, D. R., Helminiak, T. E. and Adams, W. W. *ACS Prepr., Org. Coat. Plast. Chem.* 1983, **48**, 929
7   Chuah, H. H., Kyu, T. and Helminiak, T. E. *Polymer* 1987, **28**, 2130
8   Wang, C. S., Goldfarb, I. J. and Helminiak, T. E. *Polymer* 1988, **29**, 825
9   Wang, C. S. and Bai, S. J. *Mater. Res. Soc. Symp. Proc.* 1989, **134**, 559
10 Tsai, T. T., Arnold, F. E. and Hwang, W.-F. *ACS Polym. Prepr.* 1985, **26**, 144
11 Bai, S. J., Dotrong, M. and Evers, R. C. *J. Polym. Sci., Polym. Phys. Edn* 1992, **30**, 1515
12 Heitz, T., Rohrback, P. and Hocker, H. *Makromol. Chem.* 1989, **190**, 3295
13 Ballauff, M. *Macromolecules* 1986, **19**, 1366
14 Dotrong, M., Dotrong, M. H. and Evers, R. C. *Polymer* 1993, **34**, 727
15 Vakil, U. M., Wang, C. S., Dotrong, M. H., Dotrong, M., Lee, C. Y.-C. and Evers, R. C. *Polymer* 1993, **34**, 731
16 Berry, G. C., Metzger, P. C., Venkatraman, S. and Cotts, D. B. *ACS Polym. Prepr.* 1979, **20**, 42
17 Fratini, A. V., Lenhert, P. G., Resch, T. J. and Adams, W. W. *Mater. Res. Soc. Symp. Proc.* 1989, **134**, 431
18 Alexander, L. E. 'X-ray Diffraction Methods in Polymer Science', John Wiley & Sons, New York, 1969, Ch. 7